of active damping is that the gyro always damps in with the same side up, and it probably would be best to omit fine damping and depend on either calibrating out the gyro marking error, using stutter shutdown, reducing the hemispheric-torquing moments at the end of the damping time so that the spin-axis is driven toward the maximum axis more than toward the effective pole of the markings, or using magnetic damping in connection with hemispheric torquing. Without fine damping, the complexity of the associated electronics for damping would be greatly reduced, because a sizable fraction of the electronics used in this experiment is already included in an ESG for initial spin-up and for spin-axis readout.

References

[1] Parkinson, B. and Lange, B., "The Active Damping of Free-Rotor Gyroscopes During Initial Spin-up," *Journal of Spacecraft and Rockets*, Vol. 7, No. 6, June 1970, pp. 667–675.

[2] Parkinson, B. and Lange, B., "The Active Damping of Free-Rotor Gyros," SUDAAR Report 260, May 1966, Dept. of Aeronautics and Astronautics Guidance and Control Lab., Stanford Univ.

[3] Skilling, H. H., *Electromechanics*, Wiley, New York, 1962, p. 369.

[4] Hardy, A. C. and Perrin, F. H., *The Principles of Optics*, McGraw-Hill, New York, 1932, p. 508.

[5] Planck, R. V., "Optical Flat Placement on Almost Spherical Gyro Rotors," Engineer's thesis, Aug. 1965, Dept. of Aeronautics and Astronautics, Stanford Univ.

[6] Baker, D. H. and Harrill, J. W., "Basic Principles of Unconventional Gyros," M.S. thesis, May 1954, Massachusetts Institute of Technology.

[7] Lange, B., "The Unsupported Gyroscope," *Proceedings of the 1964 Unconventional Inertial Sensors Symposium*, New York, Nov. 1964.

JUNE 1970 J. SPACECRAFT VOL. 7, NO. 6

Mariner Limit Cycles and Self-Disturbance Torques

B. Dobrotin* and E. A. Laumann†
Jet Propulsion Laboratory, Pasadena, Calif.

AND

D. Prelewicz‡
California Institute of Technology, Pasadena, Calif.

Details of the Mariner attitude control system limit cycle operation during cruise are presented. Limit cycle operation is shown to vary from the ideal case to single side operation. The data are analyzed to determine the form of the variation and to seek an explanation. The results show that there is a bias torque of several dyne-cm which changes at the end of a limit cycle, coinciding with the firing of an attitude control jet. Diagrams illustrate the various limit-cycle operations and the changes encountered. Because Mariner V had a balanced sun profile, the solar bias was low and it appeared that much of the disturbance torque was self-generated. An analysis of the attitude control jets demonstrated that a sizable torque could be generated by leakage through the attitude control valves. Experimental data obtained confirmed this suspicion.

Nomenclature

A = nozzle throat area
F = force (thrust)
G = gravitational acceleration
I_{sp} = specific impulse of jet
k = Boltzman constant
l = jet couple length
m = mass of molecule
$\dot{M}$ = mass flow rate
n = molecules number density
n_v = molecular number density having a velocity, v
$\dot{N}$ = molecular number rate
P = pressure
T = temperature
$v,\bar{v}$ = molecular velocity and average molecular velocity
$\dot{V}$ = gas volumetric flow rate
λ = mean free path length
ρ = gas density
θ = angle between nozzle centerline and molecular velocity vector
ψ = nozzle expansion half angle
σ = molecular collision cross section
τ = attitude control torque
ϕ = momentum of molecule

Subscripts

0 = all molecules
1 = molecules that do not impact nozzle
2 = molecule that impacts nozzle
s = gas supply conditions

Presented as Paper 69-844 at the AIAA Guidance, Control and Flight Mechanics Conference, Princeton, New Jersey, August 18–20, 1969; submitted August 18, 1969; revision received March 9, 1970. This work presents the results of one phase of research carried out at the Jet Propulsion Laboratory, California Institute of Technology, under Contract NAS 7-100, sponsored by NASA.

* Project Engineer, Spacecraft Control Section, Guidance and Control Division. Member AIAA.

† Member, Technical Staff, Environmental Sciences Division. Member AIAA.

‡ Doctoral candidate.

Introduction

THE Mariner series of spacecraft is designed for trips to Venus and Mars. Since 1962, five Mariners have been successfully launched; two were sent to Venus and three

have been sent to Mars. Flight times are approximately 3–4 months to reach Venus and 5–8 months to reach Mars. The primary purpose of these missions is to obtain flyby planetary data, with interplanetary data being of secondary importance. Since the scientific instruments must be aimed at the planet, three-axis stabilization is required. In addition to the requirement for stabilization at planet encounter, the solar panels, which provide electrical power during transit, must be pointed at the sun. Arbitrary attitude stabilization for midcourse maneuvers must also be provided. A detailed description of the attitude control is presented in Ref. 1.

The spacecraft attitude is controlled on three orthogonal axes: pitch, yaw, and roll. The spacecraft roll axis is (ideally) oriented along the spacecraft-sun line, and attitude control pitch and yaw is referenced to the sun. Deviation of the roll axis from the spacecraft-sun line is sensed in pitch or yaw by a cruise sun sensor; the error signal generated is fed to the control electronics. If the error signal exceeds a given level (either positive or negative: the range, positive to negative, is termed the "deadband"), a switching amplifier in the electronics activates a solenoid valve in the gas subsystem. When this valve is opened, dry nitrogen gas at low pressure flows through a small nozzle located at the end of a solar panel, thus applying torque to the spacecraft in a direction that tends to reduce the error signal. Hence, sunline orientation is maintained in pitch and yaw within the deadband, and the spacecraft is said to limit cycle within the deadband.

The spacecraft roll axis is referenced to the star Canopus, and the Canopus sensor senses angular deviation from the star and generates an error signal for roll control similar to that of a sun sensor for pitch and yaw control. Spacecraft position is thus controlled by the sun and Canopus sensors.

Spacecraft rate, in the cruise mode, is controlled by feeding back to the switching amplifier input a voltage proportional to the time a solenoid valve has been activated. This "derived rate" feedback permits the gyros in the gyro control assembly to be turned off when all celestial references have been acquired. Prior to cruise mode acquisition, these pitch, yaw, and roll-rate gyros provide rate damping to the spacecraft, enabling rapid acquisition of the sun and Canopus. Should sun or Canopus acquisition be lost, the gyros will normally be turned on to expedite the reacquisition process. A generalized single-axis attitude control subsystem is shown in Fig. 1.

The cruise attitude is shown in Fig. 2. For a Venus mission, Z of the standard XYZ spacecraft fixed coordinate system is coincident with the sun vector S. For a Mars mission, $-Z$ of the standard XYZ spacecraft fixed coordinate system is coincident with S. Deviations from this nominal attitude are measured by position sensors mounted on the spacecraft. Rotations about the X axis (pitch) and the Y axis (yaw) are measured by the sun sensors which initiate error signals related to the rotations. The Canopus sensor measures rotation about the Z axis (roll) and is affected by

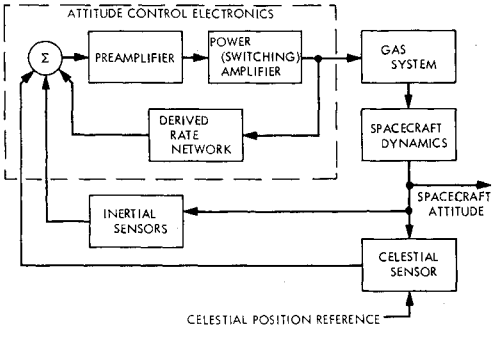

Fig. 1 Single-axis attitude control system.

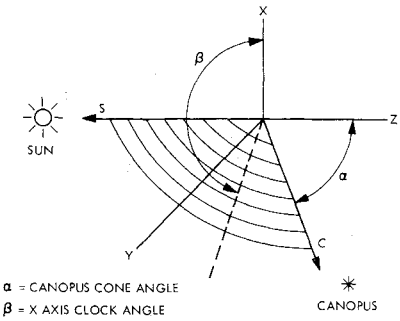

Fig. 2 Mariner coordinate reference system.

rotations in pitch and yaw. Canopus never differs from X by more than approximately 15°. This angle changes during flight as the direction of Canopus changes in relation to the spacecraft. For purposes of attitude control, the measurement is used along with measurements of the sun sensors to establish angular position deadbands. When the spacecraft rotates to the edge of a deadband, cold-gas thrusters are fired for a fixed minimum time (nominally 20 msec), applying a restoring torque about the X, Y, or Z axis, depending upon which deadband limit was reached. If there are no null offsets in the sensors, the deadbands are centered on the nominal attitude and are approximately 1° wide for pitch and yaw and $\frac{1}{2}$° wide for roll for Mariners IV and V.

Limit Cycles

Limit cycle motion is controlled by the spacecraft dynamics and the torques acting on the spacecraft as presented in the following equation:

$$T = J\dot{\omega} + \omega \times J\omega \qquad (1)$$

where T is the vector torque, ω is the spacecraft angular velocity about the center of mass as seen from an inertial reference, and J is the inertia matrix.

A theoretical single-axis limit cycle with no disturbance torques and symmetrical initial conditions is shown in Fig. 3a as a reference. In this theoretical cycle, it is assumed that the incoming rate (slope) is equal to half the minimum rate increment supplied by the attitude control system. Thus, from a simple momentum exchange, the limit cycle rate after the valve firing is equal and opposite in sign to the incoming rate. Figure 3b shows the effect of an initial limit cycle rate greater than half the minimum impulse bit. The resultant limit cycle is skewed, but the total change in angular momentum of the spacecraft is still equal to the angular momentum (impulse) imparted by the attitude control system. The motion of the spacecraft while the attitude control system is firing is not shown since the ratio between the firing time and the time between firings is approximately 10^5.

Figure 3c shows a theoretical limit cycle where there is a constant bias torque acting on the spacecraft in addition to

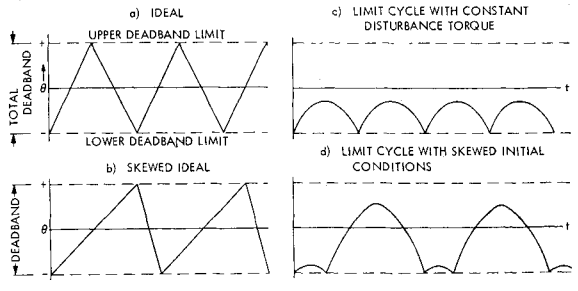

Fig. 3 Limit cycles.

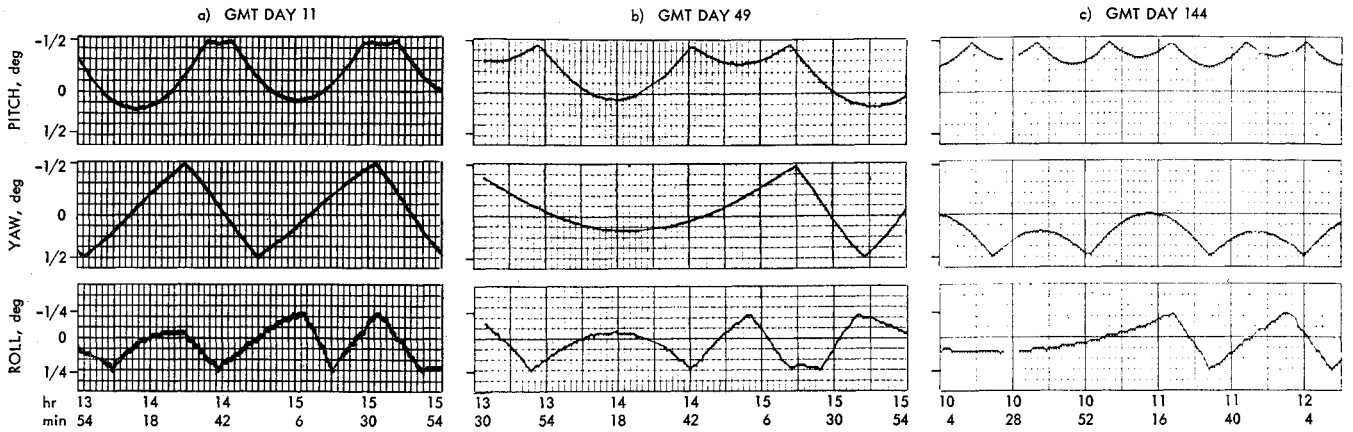

Fig. 4 Mariner IV limit cycles.

the attitude control torque. Again, symmetrical initial conditions are selected and the disturbance torque is large enough to keep the spacecraft attitude trajectory from reaching the other side of the deadband. As expected, the trajectory described is a parabola, with the time between valve firings inversely proportional to the square root of the disturbance torque

$$T_d = 8J\Delta\theta/(\Delta t^2) \qquad (2)$$

where $\Delta\theta$ is the height of the parobola, Δt is the time between attitude control switchings, and T_d is the disturbance torque. Figure 3d shows the same disturbance torque for unsymmetrical initial conditions.

The limit cycle information received from the Mariners is in the form of position versus time and is presented in this manner. This information is measured by the control position sensors. Transmittal of the data is accomplished by a digital telemetry system. At the beginning of a Mariner mission, when the spacecraft is near the Earth, data are sent at a high rate ($33\frac{1}{3}$ bits/sec). Approximately 40 days into the mission, the rate is cut to $8\frac{1}{3}$ bits/sec. During cruice mode operation, the output of the position sensors is sampled every 12.6 sec when transmission is at $33\frac{1}{3}$ bits/sec (50.4 sec when transmission is at $8\frac{1}{3}$ bits/sec). The output is converted to a 7-bit data word (DN, a binary number between 0 and 127) by a data encoder on the spacecraft and sent via the telemetry channel to tracking stations of the Deep Space Network. Before the spacecraft is flown, the position sensors are calibrated to determine the angular position-DN relationship. For calibration purposes, DN can be considered to be a continuous variable (which is later rounded off to an integer value by the data encoder). The value of DN corresponding to a number of angular displacements of the sun sensor (13 for Mariner V) is determined, and a polynomial is fitted to these points for calibration purposes.

In addition to being sampled, the raw data are also quantized, since only integer values of DN are sent via the telemetry. Hence, a given DN indicates that the angular position is within some interval. For example, a DN of 64 in the pitch channel for Mariner V indicates that the angular position is between -0.0944 and $+0.1488$ mrad, a range corresponding to DN = 64.5 and DN = 63.5, respectively, on the calibration curve.

Typical Mariner limit cycles are shown in Fig. 4 and is for Mariner IV while Fig. 5 represents Mariners VI and VII. Mariner IV was flown to Mars in 1964–1965 and Mariners VI and VII were on a Mars flyby in 1969. As will be noted, the roll channel data are more noisy than the pitch and yaw data, so that all observations are held to the pitch and yaw channels.

Figure 4a shows the type of limit cycles described previously, in that pitch has a constant bias torque while the yaw channel has almost no bias torque. The data are taken on GMT day 11 which corresponds to the 44th day of the mission. The rate increment on the yaw channel is about 88 mrad/hr (24 μrad/sec) which is a nominal value. The disturbance torque on pitch is approximately 15 dyne-cm and is constant for the period shown. The parabolas are of different height because of the initial conditions.

The length of some of the limit cycles is shown in Fig. 4b. Yaw has developed a disturbance which, in the limit cycle shown, may be approximated as 2.5 dyne-cm, while the pitch torque has dropped by approximately 10 dyne-cm. A disturbance torque of several dyne-centimeters is very difficult to measure accurately because inertia cross-coupling may affect the limit cycle motion. The period shown is in the 82nd day of flight.

On the 177th day of the mission (Fig. 4c), it may be seen (although the resolution is poor) that the pitch disturbance torque has increased to approximately 20 dyne-cm. Poor resolution is typical for high-torque levels. At the same time, the disturbance torque in yaw has reversed sign and increased to approximately 12 dyne-cm.

Figure 5 is an example of unusual changes in the limit cycles of Mariners VI and VII. Figure 5a shows both the effects of "multiple pulsing," i.e., receiving more than the

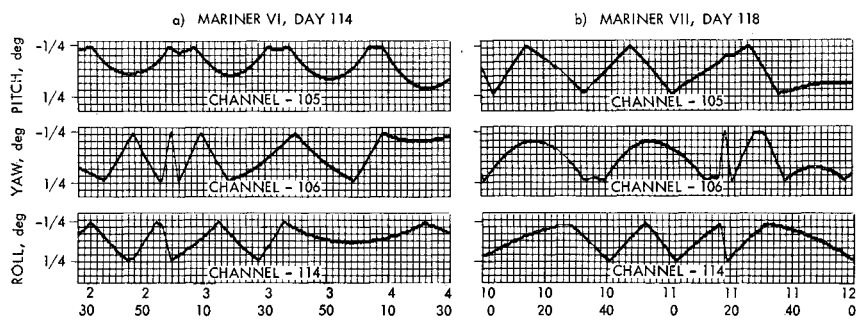

Fig. 5 Mariner VI and VII limit cycles.

minimum on time pulse, as well as a change in the disturbance torque levels in yaw and roll. The inertia interaction between the two channels is shown as well as the transition from a low disturbance torque, producing a nearly ideal limit cycle, to a higher disturbance torque, producing a one-sided limit cycle. Figure 5b shows Mariner VII, which was launched 30 days after Mariner VI. The figure shows that, for identical spacecraft, the disturbance torques can be of opposite signs. More interaction between axes during periods of high rates is shown.

Limit Cycle Analysis

The data sent back from the Mariners show the type of environment in which the attitude control system must operate during the cruise phase. However, because of the quantized nature of the data and the inertia cross-coupling between control axes, a detailed analysis of the data is required to establish definite disturbance torque levels and to discern the points at which the disturbance torque changes. Reference 2 presents an analysis of this type and is summarized here.

At this point, a single value (rather than an interval) for the angular displacement could be obtained from the calibration curve by assuming that the DN of the telemetry data is exact. The angular displacement would then assume values from a discrete set; the values would, however, be contaminated with quantization errors. These data could be processed to obtain displacements in the XYZ system. When limit cycle curves are fitted to these data, quantization errors would be expected to average out. This is true to some extent, and this is one of the procedures used in the data reduction.

Alternatively, the same computation is done using interval analysis. The displacements are then characterized by an ordered pair corresponding to the interval limits discussed earlier. Several advantages of using interval analysis are as follows. The intervals are overlapped to account for inaccuracies in data acquisition. For example, since the data encoder cannot round off exactly, there is a range of variables which may round off either way. Also, there is electrical noise in the sensor output (especially the Canopus sensor) which can cause transmission of an erroneous DN. In the example of the Mariner V pitch channel, interval overlapping results in the association of displacement interval [+0.1659 mrad, −0.1114 mrad] (corresponding to DN = 63.43 and 64.57, respectively, on the calibration curve) with a DN of 64. Other pitch and yaw displacement intervals are also overlapped by the amount cited in this example.

Consider limit cycle segments terminated by an attitude control thruster firing on any one of the three axes. As a starting point for the analysis, it is assumed that T is constant during each such segment. Equation (1) then implies that the limit cycle segments are parabolas. Subsequently, it will be established that there is, in fact, a restoring torque and, therefore, this assumption is not strictly valid. However, this restoring torque is small enough to be treated as a perturbation on the general parabolic nature of the limit cycle segments. When parabolas were fitted to these segments by least squares and by interval analysis, the following was observed: 1) The residuals of the least-squares fit appear to have the character of quantization error only. 2) The limit cycles were never so "nonparabolic" that no parabola could be fitted through all the intervals used.

It can also be inferred that the disturbance torque component about any one axis does not change significantly during a complete limit cycle on that axis. However, a thruster firing on any axis applies a significant torque to the other two axes via inertia cross-coupling and thruster misalignment. Hence, the complete limit cycles are not parabolic. If the misalignments were known, the torque input due to firings on each axis could be determined and the data adjusted to make the limit cycles appear parabolic. However, since there is no information at this time regarding thruster misalignment, the rotational motion was reconstructed by fitting parabolas to the limit cycle segments. For purposes of ordinary analysis, the standard least-squares method of curve fitting was used.

Since many of the segments do not contain enough points for a meaningful curve fit, the record of rotational motion contains time gaps. That is, when a limit cycle segment contained less than 16 points for data at $8\frac{1}{3}$ bits/sec, or less than 64 points for $33\frac{1}{3}$ bits/sec, the torque interval was so large (around 5 dyne-cm) that processing the data was not worthwhile.

Disturbance Torques for Mariners IV and V

The first conclusion that can be drawn is that a restoring torque of approximately $\frac{1}{8}$ dyne-cm/mrad is present on the pitch and yaw axes; i.e., a torque proportional to the angular displacement reaches a magnitude of 1 dyne-cm at the edge of the deadband. The presence of this restoring torque is established by considering a long limit cycle which is divided into a number of limit-cycle segments by firings on the other axes. These are shown in Ref. 2. The two middle segments have rms torque levels that are approximately 1 dyne-cm less than those of the end segments. This pattern is consistent on all such long limit cycles. This restoring torque may be attributed to the solar vanes described in Ref. 1.

There also appears to be a bias torque (some part of which is probably a solar bias torque) that changes in what appears to be a random manner from one limit cycle to the next. Relatively large changes in bias torque over long periods can be noted by comparing the torque levels with those obtained some three months later. The change is the most apparent for the pitch axes, where a change of approximately 15 dyne-cm occurred.

For Mariner V, the restoring torque appears to be much smaller than that for Mariner IV. One is tempted to assert that the presence of such a restoring torque can be deduced from the data. However, if such a restoring torque does exist, it is smaller than the resolution of this data reduction procedure. Changes in torque level on the order of a 1 dyne-cm were noted to coincide with valve firings. Not enough data were processed for Mariner V to detect long-term changes in torque level such as those which occurred on Mariner VI. A more detailed analysis of the long-term changes in torques on Mariner V is presented in Ref. 3.

In summary, Mariner IV has a comparatively large ($\sim$25 dyne-cm), slowly varying bias torque (apparently a solar torque) as well as a smaller component which changes with control valve firings; this change may be as high as from 3–5 dyne-cm. Mariner V is symmetrical about the sun line and, hence, does not have a large bias solar torque. Since there are no solar vanes, the solar-restoring torque is also considerably smaller. However, the disturbance torque which varies randomly with valve firing (by as much as 2–3 dyne-cm), is present.

Gas Leakage Thrust

The analysis on the Mariner limit-cycle data indicates that the torque level can undergo a step change at the point where an attitude control valve fires. This obviously makes the attitude control thrusters (valve and nozzle combination) suspect as causes for the randomly varying portions of the disturbance torque. Each valve is allowed a certain maximum leak rate during acceptance test and spacecraft checkout of 3 standard cubic centimeters per hour (3 scm^3/hr) nitrogen. It has been shown that valve leakage will change as a function of actuations. This may be caused by contaminants on the metal-to-metal seat, different seating characteristics, etc.

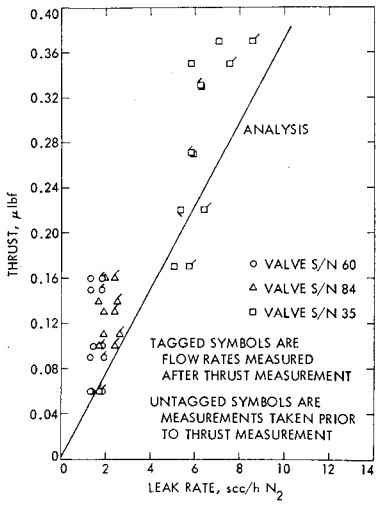

Fig. 6 Attitude control jet schematic.

However, the control valves are mounted in opposing pairs, so that opposing valves leaking at the same rate would cancel out any disturbance torques. Thus, the question is not only whether thrust is produced at a low flow rate ($\sim$3 scm^3/hr) but whether such thrust is great enough so that changes in the differences between valve pairs can account for the disturbance torques.

Because of the low leakage rates involved and the space environment in which the attitude control jets operate, the nitrogen gas flow is assumed to be in the free-molecular gas-dynamic regime. A relatively small amount of theoretical work has been done on the thrust produced by very low-density (flow rate) jets. Information is available in the literature[4] concerning the kinetic theory of gases in the free-molecular regime such that, with some reasonable assumptions and approximations, an estimation of the thrust of low-density jets can be made. The following assumptions are made: 1) the plenum of the jet is a low-pressure source of molecules; 2) the number density of molecules in the plenum is in equilibrium, i.e., the number of molecules leaking through the valve into the plenum is just equal to the number of molecules flowing out through the throat; 3) the mean free path is greater than the diameter of the throat; 4) the motion of the molecules in the plenum is Maxwellian; and 5) the thermal mass of the jet plenum and nozzle hardware is much greater than the flowing molecules. Therefore, the gas molecules entering the plenum very quickly attain the temperature of the jet hardware. Accepting these assumptions and using Fig. 6 as a guide, the problem can now be analyzed as though the plenum and throat produced a molecular beam.

The number rate of molecules which escape the plenum through the throat in all outgoing directions (as controlled by the cosine view factor) is

$$\dot{N}_0 = \frac{A}{2}\int_0^\infty v dn_v \int_0^{\pi/2} \cos\theta \sin\theta d\theta \tag{3}$$

In the jet configuration shown in Fig. 7, it should be pointed out that the molecules exiting the nozzle throat can be divided into two classes: 1) those whose direction of motion prevent them from impacting the nozzle wall, and 2) those directed toward the nozzle walls. The reason for differentiating between the classes of molecules is as follows. The number vs direction distribution of class 1 molecules is controlled by the nozzle cone angle. Because of the diffuse diffraction characteristics of molecules impacting, and emanating from the nozzle surfaces, the remaining class 2 molecules can be considered to emanate from the nozzle exit plane with a new diffuse (cosine) distribution.

The number rate of class 1 molecules is

$$\dot{N}_1 = \frac{A}{2}\int_0^\infty v dn_v \int_0^{\psi} \cos\theta \sin\theta d\theta \tag{4}$$

The number rate of remaining class 2 molecules is

$$\dot{N}_2 = \dot{N}_0 - \dot{N}_1 = [1 - (\dot{N}_1/\dot{N}_0)]\dot{N}_0 \tag{5}$$

The passage of molecules out of the plenum produces a net change in momentum of the gas. The component of that change in momentum per molecule along the axis of the jet (all others being cancelled by axial symmetry) is

$$\Delta\Phi = mv\cos\theta \tag{6}$$

The force (thrust) produced by the escaping class 1 molecules is then obtained by combining Eqs. (4) and (6) and integrating:

$$F_1 = \dot{N}_1\Delta\Phi = \frac{Am}{2}\int_0^\infty \bar{v}^2 dn_v \int_0^{\psi} \cos^2\theta \sin\theta d\theta = \frac{Am\bar{v}^2 n}{6}(1 - \cos^3\psi) \tag{7}$$

The force (thrust) produced by the escaping class 2 molecules is then obtained by combining Eqs. (3–6), which gives

$$F_2 = \dot{N}_2\Delta\Phi = [1 - (\dot{N}_1/\dot{N}_0)](\Delta\Phi)\dot{N}_0$$
$$F_2 = (Am\bar{v}^2 n/6)\cos^2\psi \tag{8}$$

The total thrust produced is then $F_1 + F_2$;

$$F = (Am\bar{v}^2 n/6)(1 + \cos^2\psi - \cos^3\psi) \tag{9}$$

Equation (9) cannot be considered explicitly correct because of the neglect of intermolecular collisions between the different class molecules in the throat and nozzle. In fact, both experimental data and theoretical treatment in the literature show that, for the limiting case of a nozzle whose cone angle is zero (a tube), a more axially oriented distribution of molecules than the diffuse cosine distribution exists. Nevertheless, Eq. (9) should be a reasonable engineering approximation.

The mean square speed of molecules escaping the plenum is

$$\bar{v}^2 = 4kT/m \tag{10}$$

The number density of exiting molecules can be determined from Eq. (3) as $\dot{N}_0 = A/4\bar{v}n$. Therefore,

$$n = 4\dot{N}_0/A\bar{v} \tag{11}$$

From the kinetic theory, the average molecular speed, which differs from the root of the mean square speed, is

$$\bar{v} = (2.55kT/m)^{1/2} \tag{12}$$

We also recall that the mass flow rate through the nozzle is equal to the leakage rate

$$\dot{M}_0 = \rho_s\dot{V}_s = \dot{N}_0 m \tag{13}$$

Equation (14) is obtained by substituting Eqs. (12) and (13) into Eq. (11)

$$n = 4\rho_s\dot{V}_s/A(2.55\, mkT)^{1/2} \tag{14}$$

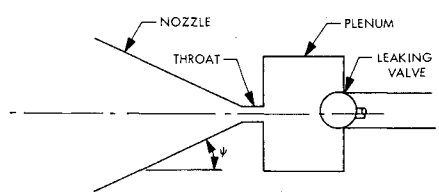

Fig. 7 Thrust vs flow.

The force (thrust) exerted by the gas exiting the jet is obtained by combining Eqs. (9, 10, and 14), as follows:

$$F = \tfrac{1}{6}\rho_s \dot{V}_s (kT/2.55m)^{1/2}(1 + \cos^2\psi - \cos^3\psi) \quad (15)$$

The specific impulse of a jet is defined as

$$I_{sp} = F/M_0 g = F/\rho_s \dot{V}_s g \quad (16)$$

i.e., by dividing Eq. (15) by $\rho_s \dot{V}_s g$.

To verify the initial assumption of free-molecular flow in the jet, the mean free path in the plenum is determined. The maxwellian mean free path is $\lambda = \frac{1}{2}^{1/2}\sigma n$, or, incorporating Eq. (14),

$$\lambda = 0.282A(mkT)^{1/2}/\sigma\rho_s \dot{V}_s \quad (17)$$

Comparison of Analytical and Experimental Results

Experiments were conducted using Mariner hardware. The gas leakage during the thrust experiments was from a nitrogen gas supply at room temperature, exhausting into a vacuum. The expansion angle of the nozzle used is 25° and the throat diam is 0.010 in. With this information, the expected performance of the jet can be evaluated. The numerical values of the necessary constants are $\rho_s = 0.00217$ slugs/ft^3, $T = 535$°R, $m = 0.318 \times 10^{-26}$ slugs, $k = 0.565 \times 10^{-23}$ ft-lb/°R, $A = 0.785 \times 10^{-4}$ in.^{2}, and $\sigma = 6.89 \times 10^{-16}$ in.^{2} Using these numerical values, the analytical relationship between the volumetric flow rate and the mean free path is $\lambda\dot{V}_s = 0.056$ in.-scm^3/hr. Using as a definition of the limit of free molecular flow that mean free path length equal to the diameter of the nozzle throat (0.010 in.), the maximum volumetric flow rate permitting free molecular flow is on the order of 6 scm^3/hr.

The analytical relationship between volumetric flow rate and the thrust is $F/\dot{V}_s = 0.0373$ μlb/(scm^3/hr).

The experimental thrust results are shown in Fig. 6 and seem to correlate reasonably well although there is some scatter in the experimental results.

Spacecraft of the Mariner class have the attitude control jets mounted on the tips of the extended solar panels and separated by ~19 ft. A disturbance torque can be evaluated as a function of the leakage flow rate such that $\Delta\tau/\dot{V}_s = \Delta F/\dot{V}_s xl/2 = 48$ dyne-cm/scm^3/hr. Thus, a difference in volumetric leakage between four coupled jets as little as 0.21 scm^3/hr can produce the 1 dyne-cm disturbance torques observed previously in flight.

Analysis indicates that the specific impulse is independent of the mass flow rate in the free molecular flow regime. The nozzle tested here should have a specific impulse of 54 sec. This value can be compared to the specific impulse of ~60 sec determined for this jet under full flight pressure flow conditions.

Conclusions

The limit cycle operation of Mariner spacecraft has been shown and the unusual behavior described. The available data have been analyzed, and show that the limit cycle operation cannot be ascribed totally to external torques (i.e., solar pressures). Further data analysis has shown that unbalanced leakage of the attitude control solenoid valves could be the cause of the varying disturbance torque. An examination of the valve-nozzle system has been made, both from an analytical and experimental standpoint, and shows that valve leakage can cause the limit cycle operation of Mariner spacecraft.

References

[1] *Mariner Mars 1964 Project Report: Mission and Spacecraft Development: Vol. I. From Project Inception Through Midcourse Maneuver*, TR 32-740, March 1968, Jet Propulsion Lab., Pasadena, Calif., pp. 214–272.

[2] Prelewicz, D. A., "Mariner IV and V Disturbances Torques and Limit Cycles," TR 32-105, Oct. 1968, Jet Propulsion Lab., Pasadena, Calif.

[3] Bourke, R. D., McReynonds, R. R., and Thuleen, K. L., "Translational Forces on the Mariner V Spacecraft Stemming from the Attitude Control System," *Journal of Spacecraft and Rockets*, Vol. 6, No. 9, Sept. 1969, pp. 1063–1066.

[4] Sears, F. W., *An Introduction to Thermodynamics, The Kinetic Theory of Gases and Statistical Mechanics*, Addison-Wesley, New York, 1950.